The EMBO Journal Vol.18 No.21 pp.5972–5982, 1999

Eps1, a novel PDI-related protein involved in ER quality control in yeast

Qiongqing Wang and Amy Chang[1]

Department of Anatomy and Structural Biology, Albert Einstein College of Medicine, 1300 Morris Park Avenue, Bronx, NY 10461, USA

[1]Corresponding author
e-mail: achang@aecom.yu.edu

PMA1 **is an essential gene encoding the yeast plasma membrane [H$^+$]ATPase. A *pma1-D378N* mutant has a dominant-negative effect on cell growth because both newly synthesized mutant and wild-type Pma1 molecules are retained and degraded in the endoplasmic reticulum (ER). Like other substrates for ER-associated degradation, Pma1-D378N is stabilized in mutants defective in components of the ubiquitination machinery. A genetic selection was performed for *eps* (ER-retained *pma1* suppressing) mutants in which the growth defect caused by the *D378N* allele is suppressed. In an *eps1* mutant, both mutant and wild-type Pma1 molecules are allowed to travel to the plasma membrane; however, normal retention of resident ER proteins Shr3 and Kar2 is not perturbed. Eps1 is a novel membrane protein belonging to the protein disulfide isomerase (PDI) family, and Eps1 co-localizes with Pma1-D378N in the ER. In the absence of Pma1-D378N, ER export of wild-type Pma1 is not affected by *eps1* deletion, but export of the plasma membrane protein Gas1 is delayed. Because Eps1 is required for retention and degradation of Pma1-D378N, we propose a model in which Eps1 acts as a novel membrane-bound chaperone in ER quality control.**

Keywords: ATPase/ER-associated degradation/molecular chaperone/plasma membrane/protein disulfide isomerase

Introduction

As the site of entry into the secretory pathway, the endoplasmic reticulum (ER) initiates the proper folding, assembly and modification of newly synthesized proteins (Hammond and Helenius, 1995). Molecular chaperones such as BiP and calnexin assist folding and assembly by preventing inappropriate interactions and/or aggregation between nascent polypeptides. In addition, protein folding in the ER is catalyzed by enzymes such as peptidyprolyl isomerase and protein disulfide isomerase (PDI) (Gething and Sambrook, 1992; Ferrari and Soling, 1999). Together, the chaperones and folding enzymes comprise a component of an ER quality control system that is designed to identify immature and abnormal proteins, thereby helping to ensure that only correctly folded and assembled proteins are released into the secretory pathway. Those newly synthesized proteins that fail to fold properly ultimately are targeted for degradation, primarily by retrograde translocation, ubiquitination and degradation by cytoplasmic proteasomes (Brodsky and McCracken, 1997; Kopito, 1997; Sommer and Wolf, 1997).

While the general concepts of ER quality control have been broadly outlined, many molecular details of the process are unknown. Genetic methods have been used to identify components of the ER-associated degradation machinery in yeast (Hampton *et al*., 1996; Knop *et al*., 1996; McCracken *et al*., 1996). While several novel genes have been identified, including *DER1*, *HRD1* and *HRD3* (Hampton *et al*., 1996; Knop *et al*., 1996), it is not known whether these gene products participate in initial events in quality control, e.g. identification of the substrate, or in subsequent events, e.g. retrograde transport to the cytoplasm for degradation. Also unanswered is the question of how the quality control machinery discriminates between normal proteins in the process of folding and misfolded proteins to be degraded, although molecular chaperones have been suggested to participate in substrate selection for ER-associated degradation (ERAD) (Brodsky and McCracken, 1997; Kopito, 1997; Sommer and Wolf, 1997).

We have studied ER quality control in *Saccharomyces cerevisiae* by examining a mutation in *PMA1*, encoding the plasma membrane [H$^+$]ATPase, which causes a defect in ER export of the newly synthesized molecule. Pma1 is a major polytopic cell surface protein whose physiological role is to regulate intracellular pH and generate an electrochemical gradient by pumping protons out of the cell. Pma1 belongs to the P-type ATPase family of ion transporters whose members have a conserved aspartate residue that undergoes phosphorylation during catalysis. Previous work to study the functional consequences of mutating the predicted catalytic phosphorylation site of *S.cerevisiae* Pma1 (Asp378) led to the discovery that a substitution at this residue causes defective delivery of the newly synthesized protein to the plasma membrane. Instead, the mutant protein is misfolded and retained in the ER (Harris *et al*., 1994; DeWitt *et al*., 1998; Maldonado *et al*., 1998; Nakamoto *et al*., 1998). Indeed, the entire region surrounding Asp378, lying in the central cytoplasmic domain bounded by 10 transmembrane segments, appears important for proper folding and ER export (DeWitt *et al*., 1998). Because Pma1 at the cell surface is essential for growth, a defect in Pma1 biogenesis causes growth arrest. The *pma1-D378N* allele, even in the presence of wild-type *PMA1*, has a dominant-negative effect on growth (Harris *et al*., 1994; DeWitt *et al*., 1998; Maldonado *et al*., 1998; Nakamoto *et al*., 1998).

We report here that Pma1-D378N undergoes degradation at the ER in a ubiquitin-dependent manner. In the presence of the mutant allele, wild-type Pma1 also undergoes retention and degradation. A genetic selection for mutants which suppress the dominant-negative growth

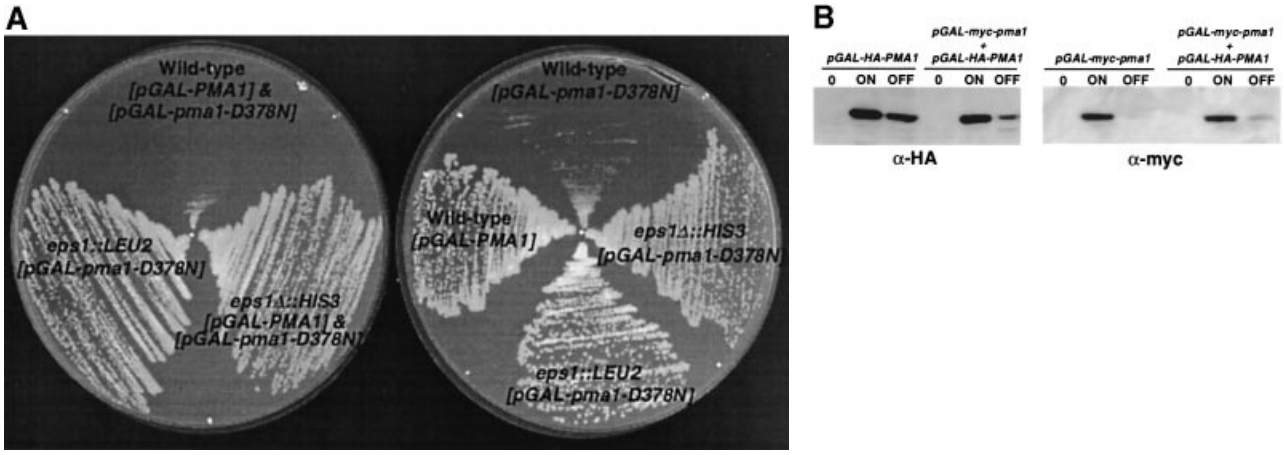

Fig. 1. Dominant-negative effect of mutant Pma1-D378N. (**A**) Growth on plates (synthetic complete medium containing 2% galactose) at room temperature. Cells (F1105) bearing *pGAL-HA-PMA1* (pXZ28) grow. Cells bearing *pGAL-pma1-D378* (pRN409) cannot grow. Cells cannot grow with both the *URA3*-marked plasmid bearing *PMA1* (pXZ28) and the *LEU2*-marked plasmid bearing *pma1-D378N* (pRN409). *eps1* permits growth of cells (WQY1) expressing Pma1-D378N. (**B**) Western blot showing induction of Pma1 and stability after shutting off synthesis. Wild-type cells (F1105) bearing *pGAL-HA-PMA1* (pXZ28) or *pGAL-myc-pma1-D378N* (pWQ2) or both plasmids were grown to log phase in synthetic complete medium containing 2% raffinose (time 0) and then transferred to medium containing 2% galactose to induce synthesis of epitope-tagged Pma1 for 4 h (on). Glucose was then added to 3% to shut off synthesis and incubation continued for 4 h (off). Cell lysate was prepared, normalized to protein for SDS–PAGE and analyzed by Western blotting using anti-HA (left panel) and anti-myc antibody (right panel). Newly synthesized Pma1-D378N is degraded while wild-type Pma1 is stable. When the plasmids bearing *PMA1* and *pma1-D378N* are co-expressed, both wild-type and mutant molecules are degraded.

effect of Pma1-D378N has resulted in identification of *EPS1* (ER-retained Pma1 suppressing). Importantly, in *eps1*Δ cells, retention of Pma1-D378N and wild-type Pma1 is reversed, and both molecules are delivered to the plasma membrane. Nevertheless, retention of the ER resident proteins Kar2 and Shr3 appears normal. In the absence of Pma1-D378N, ER export of wild-type Pma1 is not perturbed by *eps1* deletion; however, export of a wild-type membrane marker, Gas1, is delayed. *EPS1* encodes a novel membrane protein belonging to the PDI family. We propose a role for Eps1 in recognition and delivery of substrate to the ER quality control machinery.

Results

Retention and degradation of Pma1-D378N by ER quality control

The *pma1-D378N* allele has a dominant-negative effect on growth as cells expressing the mutant protein cannot grow even though there is a chromosomal copy of *PMA1* (Figure 1A and Harris *et al*., 1994). Previously, it has been suggested that mutant Pma1-D378N is retained in the ER as a consequence of a quality control mechanism (Harris *et al*., 1994; Nakamoto *et al*., 1998). To determine whether Pma1-D378N undergoes degradation, we examined the fate of the newly synthesized molecule. To monitor the mutant and wild-type proteins independently, we have employed constructs in which wild-type and Pma1-D378N were tagged with hemagglutinin (HA) and c-myc epitopes, respectively. Expression was placed under the control of a regulated promoter; *GAL1* and *MET25* promoters produced similar results (see below). In Figure 1B, cells bearing *pGAL-myc-pma1D378N* were shifted to galactose-containing medium to induce synthesis. Glucose was added to shut off synthesis. Levels of newly synthesized Pma1 were detected by Western blot (with anti-myc and anti-HA antibodies) after 4 h induction as well as a further 4 h of chase. Figure 1B shows that after chase, newly synthesized wild-type Pma1 (left panel) remains relatively stable, consistent with the long half-life of Pma1 (Benito *et al*., 1991; Chang and Fink, 1995), while Pma1-D378N is rapidly degraded (right panel). Degradation of newly synthesized wild-type Pma1 is also accelerated significantly when Pma1-D378N is expressed (Figure 1B).

Because some *pma1* mutants have been reported to escape ER quality control and undergo degradation in the vacuole (Chang and Fink, 1995), Pma1-D378N degradation was examined in *pep4*Δ cells, defective in vacuolar proteinase activity. Figure 2A shows that Pma1-D378N degradation in *pep4* cells is not inhibited with respect to that of wild-type cells. Degradation of Pma1-D378N was then examined in a *ubc6 ubc7* mutant because the ubiquitin-conjugating enzymes Ubc6 and Ubc7 are required for ERAD (Brodsky and McCracken, 1997; Sommer and Wolf, 1997). Figure 2B shows that in *ubc6 ubc7* cells, degradation of newly synthesized Pma1-D378N is slowed by comparison with that in wild-type cells. These data reveal that Pma1-D378N degradation is dependent on Ubc6 and Ubc7, but not vacuolar proteases, indicating that it is indeed a substrate for ER quality control.

Accumulation of Pma1-D378N affects ER structure and function

The observation that ER retention and degradation of Pma1-D378N causes, in turn, retention and degradation of wild-type Pma1 suggests a possible explanation for the dominant-negative growth effect of the mutant allele: wild-type Pma1 and its essential activity at the plasma membrane become rate limiting for growth. Because Pma1 turns over at the cell surface with a half-time of ~11 h (Benito *et al*., 1991), an effect on cell growth due to defective delivery of newly synthesized Pma1 is predicted to have a slow onset. Indeed, growth curves confirmed that a detectable decrease in rate of growth was first

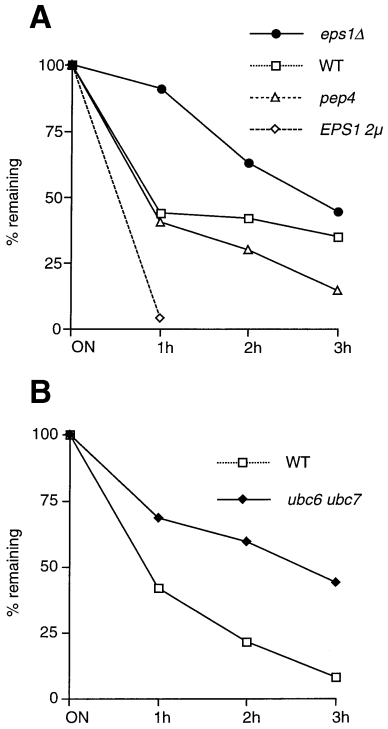

Fig. 2. Degradation of mutant Pma1–D378N. (**A**) Stability of Pma1–D378N in the presence of *pep4*Δ (WQY2), *eps1*Δ (WQY1) and multicopy *EPS1* (F1105-pWQ29). Cells bearing *pMET-HA-pma1-D378N* (pWQ12) were transferred to methionine-free medium for 2 h (time 0). Methionine was then added back and, at various times of chase, Pma1-D378N levels were quantitated by Western blot and phosphorimaging, and expressed as a percentage of induced protein. Rates of Pma1-D378N degradation are similar in wild-type (□) ($t_{1/2}$ estimated from semi-log plot ~1.28 h) and *pep4*Δ (△) cells ($t_{1/2}$ ~1.1 h). Stabilization of mutant Pma1 is apparent in *eps1*Δ cells (●) ($t_{1/2}$ ~3 h), while degradation is increased by multicopy *EPS1* (◇) ($t_{1/2}$ ~0.2 h). (**B**) Pulse–chase analysis of wild-type (sub62) (□) and *ubc6 ubc7* (MHY552) (◆) cells bearing *pMET-HA-pma1-D378N* (pWQ12). Cells were resuspended in methionine-free medium for 2 h to induce expression of Pma1-D378N, and then labeled with Expre^{35}S^{35}S for 15 min. Cells were then chased in the presence of excess methionine and cysteine for various times. Immunoprecipitation with anti-HA antibody was normalized to lysate protein, analyzed by SDS–PAGE and quantitated by densitometry. Degradation of mutant Pma1 is delayed in *ubc6 ubc7* cells ($t_{1/2}$ estimated from semi-log plot ~2.35 h) by contrast with wild-type cells ($t_{1/2}$ ~0.85 h).

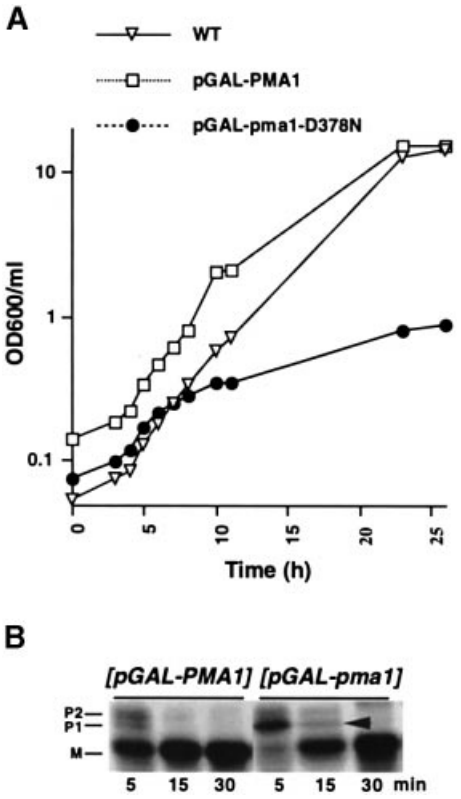

Fig. 3. Effect of expression of Pma1-D378N. (**A**) Growth of cells upon expression of Pma1-D378N. Cells exponentially growing in synthetic complete medium containing 2% raffinose were transferred to medium containing 2% galactose. Cultures were incubated at 30°C and OD_{600} measurements were made at various times. Note that there is no detectable difference in growth rate of cells bearing *pGAL-PMA1* (pXZ28) and *pGAL-pma1-D378* (pWQ2) until ⩾6 h after shift to galactose–containing medium. (**B**) Intracellular transport of CPY in cells expressing mutant Pma1-D378N. Cells bearing *pGAL-PMA1* or *pGAL-pma1-D378N* were grown in raffinose-containing medium and then shifted to galactose-containing medium for 4 h. Cells were then pulse-labeled at 30°C for 5 min with Expre^{35}S^{35}S and chased for various times. Immunoprecipitation with anti-CPY antibody was normalized to TCA-precipitable c.p.m.. The arrowhead indicates P1 CPY persisting in cells accumulating Pma1-D378N.

apparent only ⩾6 h after induction of Pma1-D378N expression (Figure 3A).

Alternatively, it is possible that the growth defect caused by Pma1-D378N accumulation is a consequence of a general perturbation of ER function. To test this, the effect of Pma1-D378N on maturation of the vacuolar protein carboxypeptidase Y (CPY) was examined by pulse–chase analysis. Newly synthesized CPY enters the secretory pathway at the ER as a 67 kDa P1 form. Further glycosylation upon transit to the Golgi produces a 69 kDa P2 form, and proteolytic processing upon arrival at the vacuole yields the 61 kDa mature enzyme (Stevens *et al*., 1982). Cells carrying *pGAL-pma1-D378N* were shifted to galactose-containing medium for 4 h, and then pulse-labeled with [^{35}S]methionine and cysteine. At this time, the growth rate is not altered detectably (Figure 3A). Figure 3B shows that in cells accumulating Pma1-D378N, there is a slight delay in maturation of P1 CPY to the Golgi P2 form, in contrast to cells expressing only wild-type Pma1 (Figure 3B, arrowhead). Delivery of the vacuolar membrane protein alkaline phosphatase was similarly slowed in cells expressing Pma1-D378N (not shown). Perturbation of ER export is dependent on accumulation of Pma1-D378N: no effect on CPY export was observed at a time prior to detectable accumulation (at 1 h after induction; not shown).

eps1 suppresses the dominant-negative growth defect induced by Pma1-D378N

To understand better the molecular basis of Pma1-D378N retention and degradation within the ER, a genetic selection was performed to isolate *eps* mutants which suppress the growth defect caused by *pma1-D378N*. Cells carrying *pGAL-pma1-D378N* were transformed with a mutagenized genomic library containing random insertions of *lacZ* and *LEU2* (Burns *et al*., 1994), and then plated on galactose-containing medium. Transformants that grew on galactose were selected. Tetrad analysis was used to identify suppressors in which the *LEU2* insertion segregated 2:2, indicating a single genetic locus, and was linked to growth on galactose medium. While several *eps* mutants were

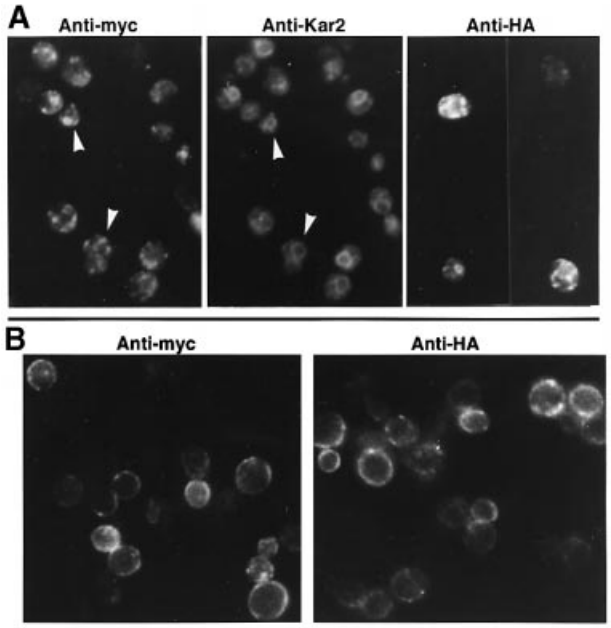

Fig. 4. Indirect immunofluorescence localization of Pma1 in wild-type and *eps1* cells expressing Pma1-D378N. Exponentially growing cells (F1105) bearing *pGAL-myc-pma1* (pWQ2) and/or *pGAL-HA-PMA1* (pXZ28) were transferred to medium containing 2% galactose. After 4 h, cells were fixed, spheroplasted and permeabilized for indirect immunofluorescence. (**A**) Co-localization of Pma1-D378N and Kar2 (top left and middle panels). Cells expressing myc-Pma1-D378N were stained with anti-myc monoclonal and polyclonal anti-Kar2 antibodies, followed by Cy3- and Cy2-conjugated secondary antibodies, respectively. Staining of myc-Pma1-D378N is frequently coincident with (arrowheads), but not identical to the staining pattern of the ER marker Kar2. Right panel: cells expressing both myc-tagged mutant and HA-tagged wild-type Pma1 were stained with anti-HA antibody. The distribution of wild-type Pma1 appears similar to that of Pma1-D378N. (**B**) Pma1 localization in *eps1*Δ cells (WQY1) expressing myc-Pma1-D378N and HA-Pma1 were stained with anti-myc and anti-HA antibodies. Staining of both wild-type and mutant Pma1 is predominantly at the cell surface.

identified that satisfied these criteria, only *eps1* cells permitted substantial synthesis of Pma1-D378N to occur. Therefore, it seemed quite likely that *eps1* affects the post-translational fate of mutant Pma1. Figure 1A shows that cells with an insertion within the *EPS1* coding sequence can grow when Pma1-D378N is expressed. A strain was constructed bearing a complete deletion and replacement of *EPS1* with *HIS3*; these cells also suppress the growth defect caused by mutant Pma1 expressed from either *GAL1* (Figure 1A) or *MET25* promoters (not shown), and were used for further analysis.

eps1 allows mutant Pma1 to move from ER to plasma membrane

To address the mechanism by which *eps1* suppresses *pma1-D378N*, the stability and localization of newly synthesized Pma1 were examined. As shown in Figure 2A, degradation of mutant Pma1 is slowed in *eps1*Δ cells; by contrast, *EPS1* overexpression increases mutant Pma1 degradation.

Localization of mutant Pma1 was studied by indirect immunofluorescence. ER retention of myc-tagged Pma1-D378N was first confirmed in wild-type cells. Figure 4A (left panel, arrowheads) shows staining of cells expressing myc-tagged mutant Pma1 from a *GAL1* promoter. Large punctate structures are stained which appear distinct from any organelle described in wild-type cells. By contrast, staining with antibody against the ER marker Kar2 revealed a predominantly perinuclear pattern, closely resembling the ER pattern reported for wild-type cells (Rose *et al*., 1989). In some cells, myc staining is coincident with Kar2 staining, indicating that mutant Pma1-D378N is retained in the ER (Figure 4A, arrowheads and Harris *et al*., 1994). There is more extensive co-localization of Pma1-D378N with Kar2 in a perinuclear distribution in cells expressing *MET-pma1-D378N* (see Figure 9), suggesting that the large punctate structures are a reflection of *GAL1*-induced protein proliferation. In the presence of the mutant allele, the localization pattern of HA-tagged wild-type Pma1 is also punctate (Figure 4A, right panel); there is no obvious staining of either mutant or wild-type Pma1 at the plasma membrane. ER retention of both mutant and wild-type Pma1 is consistent with degradation of the wild-type protein in the presence of Pma1-D378N (Figure 1B).

Co-localization of newly synthesized Pma1-D378N and wild-type Pma1 at the ER was examined further by cell fractionation. Previous work has established that Renografin density gradients efficiently resolve plasma membrane from intracellular (ER, Golgi and vacuole) membranes (Schandel and Jenness, 1994). As a control, the fractionation pattern of cells expressing *pGAL1-HA-PMA1* alone was determined (Figure 5A, panel a); HA-Pma1 is present predominantly in fractions 10 and 11, coincident with plasma membranes [detected using the plasma membrane marker Gas1 (Figure 10 below) and anti-Pma1 antibody in the absence of induced protein (not shown)]. When wild-type Pma1 is expressed together with Pma1-D378N, the HA-tagged protein shifts to fractions 7 and 8, where myc-Pma1-D378N also accumulates (Figure 5A, panels b and c). These fractions are enriched in the ER, based on their content of the ER membrane marker Sec61 (panel d).

In *eps1* cells, strikingly, localization by indirect immunofluorescence shows staining of both Pma1-D378N and wild-type Pma1 at the cell surface (compare Figure 4B with A). In agreement with the immunofluorescence results, fractionation on a Renografin density gradient shows both mutant and wild-type Pma1 migrating with the plasma membrane in fractions 10 and 11, away from the ER marker, Sec61, in fraction 7 (Figure 4B). Therefore, *eps1*Δ stabilizes Pma1-D378N by reversing its ER retention, and permitting export of both mutant and wild-type Pma1 to the plasma membrane.

Because Eps1 is required for ER retention of Pma1-D378N, further work was carried out to determine whether retention of ER resident proteins Shr3 and Kar2 is affected by *eps1*Δ. Localization of the membrane protein Shr3 (Ljungdahl *et al*., 1992) and the lumenal protein Kar2 was examined by indirect immunofluorescence. As shown in Figure 6A, both Shr3 and Kar2 are found in a typical ER distribution surrounding the nucleus [shown by 4′,6-diamidino-2-phenylindole (DAPI) staining] in *eps1* cells. Localization of both ER residents in *eps1* cells is indistinguishable from that in wild-type cells. Figure 6B shows no detectable secretion of Kar2 in *eps1*Δ and wild-type cells, by contrast with *erd2* cells which readily secrete Kar2 (Semenza *et al*., 1990). Therefore, *eps1*Δ prevents

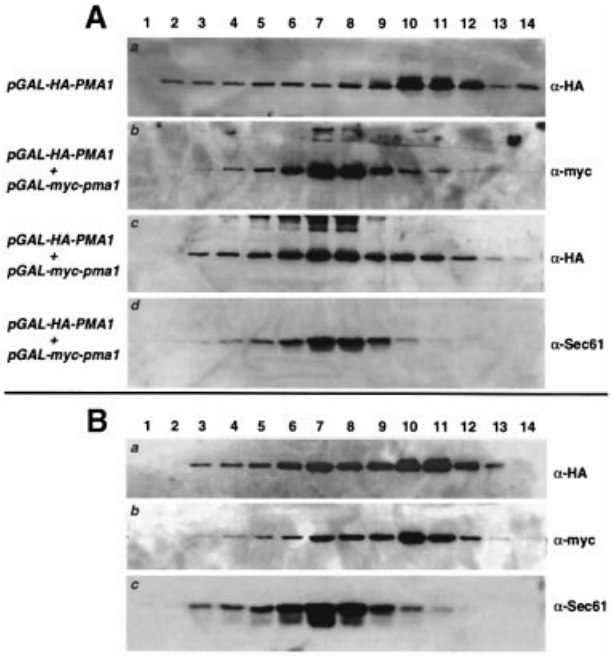

Fig. 5. Pma1 distribution in wild-type and *eps1* cells expressing Pma1-D378N by cell fractionation. Cells were transferred to galactose-containing medium for 4 h to induce Pma1 synthesis, as described in Figure 4. Cells were then lysed for fractionation on Renografin density gradients. (**A**) Distribution of Pma1 in wild-type cells. Panel a shows the distribution of HA-Pma1 in wild-type cells (F1105) expressing solely *pGAL-HA-PMA1* (pXZ28); the protein is found predominantly in fractions 10–11. In these cells, the ER marker Sec61 is found predominantly in fractions 7–8 (not shown). Panels b and c, respectively, show the distribution of myc-Pma1-D378N (pWQ2) and HA-Pma1 (pXZ28) when both molecules are co-expressed in wild-type cells. Under these circumstances, the major fraction of HA-tagged Pma1 is found in fractions 7–8, as is myc-tagged Pma1-D378N and Sec61 (panel d). (**B**) Distribution of Pma1 in *eps1*Δ cells. Fractionation of HA-Pma1 and myc-Pma1-D378N in *eps1*Δ (WQY1) cells is shown. Both proteins are found predominantly in fractions 10–11, by contrast with Sec61, which is predominantly in fraction 7.

retention of Pma1-D378N but does not affect retention of normal ER proteins.

Eps1 is a novel member of the protein disulfide isomerase-related family

The identity of the disrupted *eps1* gene was determined by cloning and sequencing genomic DNA immediately adjacent to the insertion (Burns *et al*., 1994). A database search revealed that *eps1* contained an insertion within the open reading frame corresponding to YIL005w (Cherry *et al*., 1997). BLAST analysis indicates that *EPS1* encodes a novel protein with high sequence similarity to PDI (~20% identity) and other proteins of the PDI family. Eps1 contains a domain which is common to all members of the family and is the active site of the oxidoreductase thioredoxin. The domain contains a CXXC motif that can participate in dithiol–disulfide exchange reactions (Luz and Lennarz, 1996; Ferrari and Soling, 1999) (asterisks, Figure 7A). Figure 7A shows an alignment of Eps1 with members of the PDI family identified in yeast, including Pdi1 (Gunther *et al*., 1991; LaMantia *et al*., 1991), Eug1 (Tachibana and Stevens, 1992), Mpd1 (Tachikawa *et al*., 1995) and Mpd2 (Tachikawa *et al*., 1997). Other members of the yeast PDI family are ER lumenal proteins [with HDEL signals at the C-terminus (Figure 7A)]. In contrast, hydropathy analysis of Eps1 predicts an N-terminal signal sequence and a single transmembrane domain (underlined in Figure 7A), and Eps1 terminates with the sequence KKKNQD, which fits closely the consensus motif for retention of transmembrane proteins in the ER (Jackson *et al*., 1990).

While *PDI1* is essential for cell viability, *EPS1* and other members of the family are not. Indeed, *eps1*Δ does not cause any detectable growth defect (not shown). Overexpression of other yeast PDI family members allows cells to grow in the absence of *PDI1* (Tachibana and Stevens, 1992; Tachikawa *et al*., 1995, 1997). A plasmid shuffle experiment was performed to determine whether *EPS1* overexpression can suppress lethality of *pdi1*Δ. For this purpose, a strain was employed in which a chromosomal deletion of *PDI1* is complemented by the *PDI1* gene on a *URA3*-marked plasmid. These cells cannot live without the plasmid and cannot grow on 5-fluoro-orotic acid (5-FOA) (Boeke *et al*., 1987). The ability of high copy *EPS1* to replace the *URA3*-marked plasmid bearing *PDI1* was assayed by growth on 5-FOA. As a positive control, the ability of *EUG1* overexpression to suppress the lethality of *pdi1*Δ was tested. Figure 7B shows that *EPS1* overexpression, like that of *EUG1*, allows *pdi1*Δ cells to grow on 5-FOA in the absence of *PDI1*.

Because Eps1 can replace the essential function of PDI, it was of interest to assess whether Eps1 also plays a role in disulfide bond formation of newly synthesized proteins. Previous work has demonstrated that disulfide bond formation is required for proper folding and ER export of CPY (Tachibana and Stevens, 1992). Therefore, we examined intracellular transport of CPY in *eps1* cells. Figure 8 shows that there is no discernible difference in the kinetics of appearance of P1, P2 and M forms of CPY in wild-type and *eps1*Δ cells. Specifically, accumulation of the P1 or ER form of CPY in *eps1* cells was not detected. These data indicate that Eps1 is not required for disulfide bond formation and ER export of CPY.

In order to characterize Eps1, we employed a construct tagged with the c-myc epitope at the C-terminus before the KKKNQD sequence; this construct behaves like wild-type Eps1 in its ability to reverse suppression of *pma1–D378N* as well as complementing the *eps1*Δ phenotype (described further below). By Western blot (Figure 9A), myc-tagged Eps1 is seen as a faint single band of M_r ~88 kDa, slightly larger than predicted by its sequence. The intensity of the signal increases substantially when tagged *EPS1* is expressed from a high copy plasmid. Upon fractionation of lysate, Eps1 is associated with a membrane pellet isolated following centrifugation at 10 000 *g*. Because Eps1 remains associated with membranes after extraction with 0.5 M NaCl or 0.1 M Na carbonate, pH 11.5 (Figure 9A), we conclude that Eps1 behaves as an integral membrane protein (Steck and Yu, 1973). Localization of Eps1 was then determined by indirect immunofluorescence. Figure 9B shows the staining of *eps1*Δ cells bearing multicopy myc-tagged *EPS1*. (Specific staining of the construct on a centromeric plasmid was not detectable.) Staining of myc–Eps1 is coincident with perinuclear Kar2 staining in some cells (Figure 9B, arrows). In the presence of Pma1-D378N, there is some co-localization of Eps1 and mutant Pma1. Additionally,

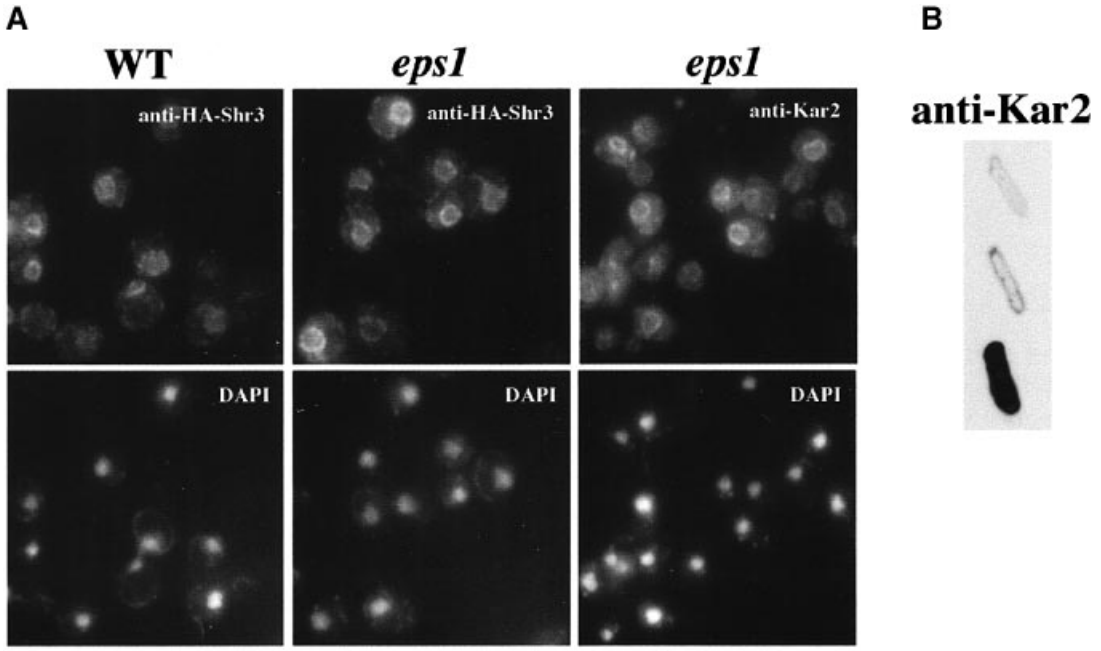

Fig. 6. Retention of ER proteins. (**A**) Localization of ER resident proteins Shr3 and Kar2. Indirect immunofluorescence staining with anti-HA and DNA staining with DAPI were performed in wild-type (F1105) and *eps1* (WQY1) cells bearing *HA-SHR3* (B2513). Staining with anti-Kar2 antibody was performed in *eps1* cells. (**B**) Kar2 secretion assay. Western blot with anti-Kar2 antibody of nitrocellulose filter overlying wild-type, *eps1* and *erd2* (MY3331) cells. Only *erd2* cells secrete Kar2.

there is punctate Eps1 staining in the cytoplasm that is distinct from both Kar2 and Pma1-D378N staining.

Effect of eps1 on protein export from the ER

The effect of *eps1* on intracellular transport of wild-type Pma1 was examined in the absence of Pma1-D378N. Previously, it has been shown that under conditions in which ER export of Pma1 is impaired, Pma1 accumulation at the ER can be detected (Roberg *et al*., 1999). Therefore, the distribution of wild-type Pma1 in *eps1* cells was studied by density gradient fractionation. Figure 10 shows that in both *eps1* and wild-type cells, Pma1 is found in plasma membrane-enriched fractions 10 and 11 (panels a and b). Similarly, by indirect immunofluorescence, Pma1 appears localized exclusively to the plasma membrane in both *eps1* and wild-type cells (not shown).

Strikingly, although no effect of *eps1* on wild-type Pma1 transport was detected, ER accumulation of the plasma membrane protein Gas1 was observed. Insertion of Gas1 into the ER membrane occurs via a GPI anchor and is accompanied by core glycosylation, generating an M_r 105 kDa form. Movement to the Golgi is rapid and Gas1 shifts to 125 kDa as it acquires further glycosylation (Doering and Schekman, 1996; Sutterlin *et al*., 1997). Figure 10 shows Gas1 distribution after density gradient fractionation (panels c and d). In wild-type cells, Gas1 is predominantly at the plasma membrane (fractions 10 and 11). By contrast, in *eps1*Δ cells, there is accumulation of the 105 kDa ER form of Gas1 in lower density (7 and 8) fractions (arrowhead, panel c). Pulse–chase analysis revealed a delay in generation of the 125 kDa Golgi-modified form of Gas1 in *eps1*Δ cells by comparison with wild-type cells, consistent with the idea that slowed ER export results in ER accumulation (not shown). These data suggest that Eps1 does not play an important role in ER export of wild-type Pma1, but facilitates export of Gas1.

Discussion

The Pma1-D378N mutant is misfolded, retained and accumulated in the ER (Figures 4 and 5; Harris *et al*., 1994; DeWitt *et al*., 1998; Maldonado *et al*., 1998; Nakamoto *et al*., 1998). Pma1-D378N is a substrate for ER quality control as its degradation is dependent on Ubc6 and Ubc7, but not Pep4 (Figure 2). Both mutant and wild-type Pma1 are retained and degraded concomitantly (Figure 1). Recent evidence that Pma1 forms a hexamer (Auer *et al*., 1998) supports a model in which oligomerization of mutant and wild-type Pma1 in the ER results in retention and degradation of both molecules.

We suspect that the growth defect associated with Pma1-D378N accumulation is accounted for by a block in Pma1 export coupled with gradual depletion of Pma1 enzyme activity from the cell surface. This idea is supported by a decrease in growth rate that is detectable only $\geqslant$6 h after induction of Pma1–D378N expression (Figure 3), consistent with the slow rate of Pma1 turnover at the plasma membrane (Benito *et al*., 1991). Even so, at a time when growth is not yet significantly affected, Pma1-D378N accumulation begins to cause moderate disturbances of ER structure and function. By 4 h after induction, both mutant and wild-type Pma1 were observed in large punctate structures (Figure 4); these structures may represent proliferated ER membrane, as has been reported upon overproduction of various membrane proteins (reviewed in de-Kerchove d'Exaerde *et al*., 1996). In addition, export of newly synthesized proteins from the ER is perturbed in cells that accumulate Pma1-D378N (Figure 3). In contrast with the complete block of export of wild-type

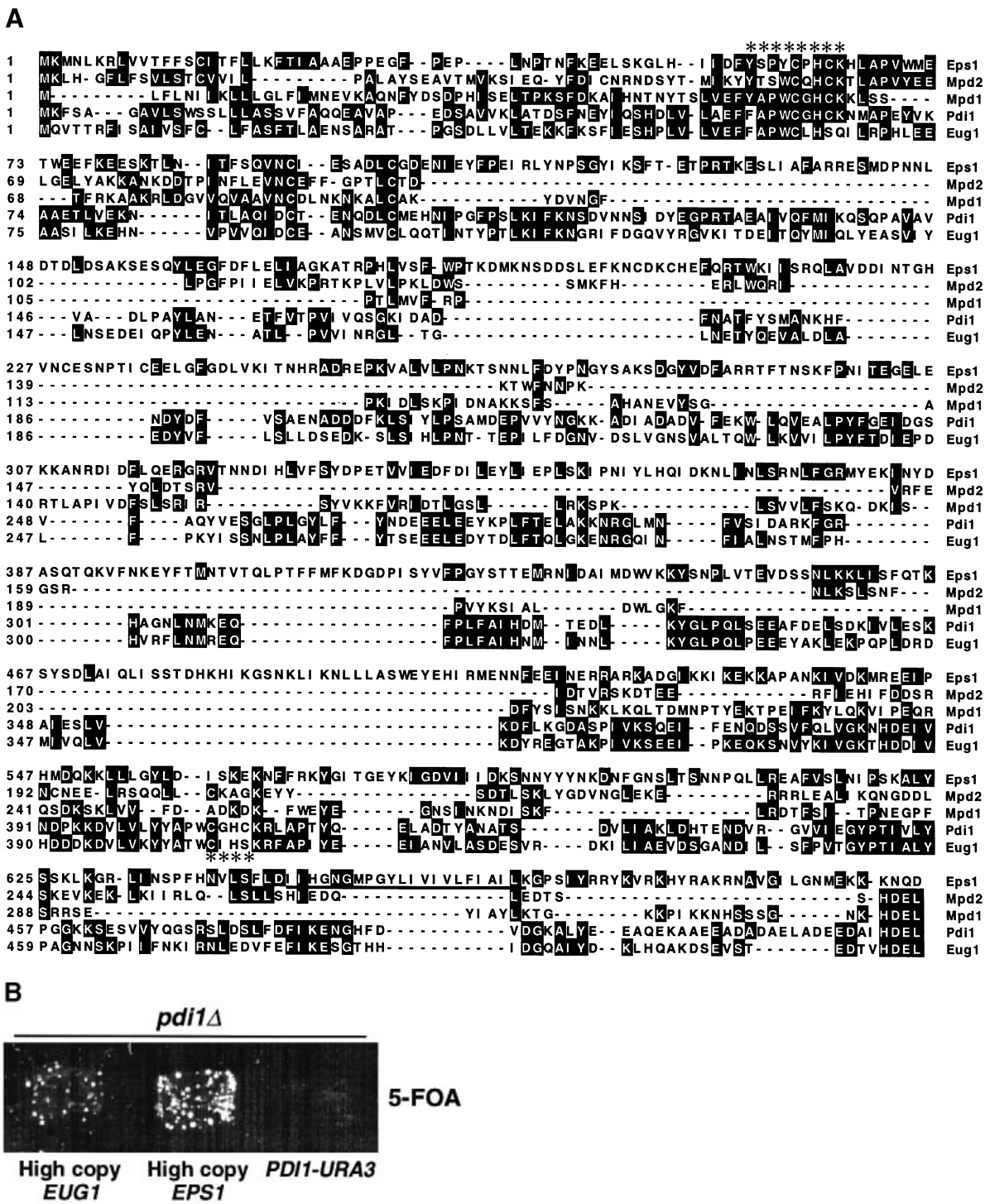

Fig. 7. Eps1 is a member of a family of proteins related to protein disulfide isomerase. (**A**) Alignment of Eps1 with other members of the yeast PDI family. Sequences were aligned using the MegAlign program (DNAstar, Madison, WI) using the Clustal method (Higgins *et al*., 1992). Identical amino acid residues are boxed, and hyphens indicate gaps introduced to maximize alignment. Asterisks overlie conserved thioredoxin-like CXXC motifs; PDI has two while Eps1 has a single thioredoxin-like domain. All members of the family, except Eps1, have HDEL retention signals at the C-terminus; Eps1 terminates with the residues KKKNQD at the C-terminus. The predicted transmembrane domain is underlined. (**B**) Overexpression of *EPS1* can suppress the lethality of *pdi1*Δ. A strain with a chromosomal deletion of *PDI1* complemented by *PDI1* on a *URA3*-marked plasmid was transformed with multicopy *EPS1* (pWQ19) or *GAL1-EUG1* (pCT44). After growth in medium containing galactose and uracil, Ura$^-$ cells were selected on 5-FOA. Overexpression of *EUG1* and *EPS1* suppresses the lethality of *pdi1*Δ.

Pma1, there is only a kinetic slowing in export of other proteins. Indeed, this effect is likely to be a consequence of Pma1 accumulation because it was not detected at early times after induction.

A major finding in this study is the identification of *EPS1* in a genetic selection for suppressors of *pma1-D378N*. Many of the previous genetic screens to identify components of the yeast ER quality control apparatus have isolated mutants that prevent degradation of a substrate, leading to identification of components of the degradation

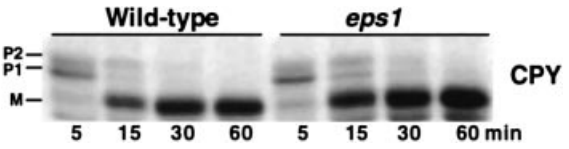

Fig. 8. Effect of *eps1* on maturation of CPY. Wild-type (F1105) and *eps1*Δ (WQY1) cells were pulse-labeled for 5 min at room temperature with Expre^{35}S^{35}S and chased for various times. Immunoprecipitation of CPY from lysates was normalized to acid-precipitable c.p.m. The kinetics of CPY maturation in wild-type and *eps1* cells are similar.

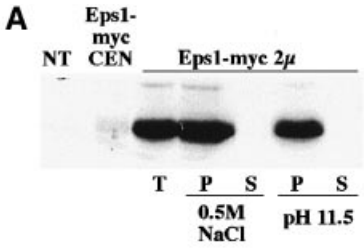

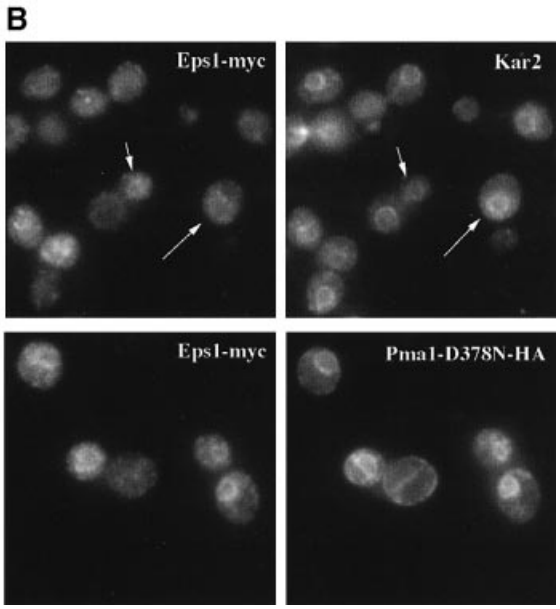

Fig. 9. Eps1 is an ER membrane protein. (**A**) Western blot. Lysate was prepared from *eps1*Δ cells (WQY1) with or without a centromeric or 2μ plasmid bearing myc-tagged *EPS1* (pWQ28 and pWQ30), and mixed with an equal volume of 1 M NaCl or 0.2 M Na carbonate, pH 11.5. After incubation on ice for 30 min, the sample was centrifuged at 100 000 *g* for 1 h to generate soluble and membrane fractions. The presence of Eps1 in total (T), supernatant (S) and pellet (P) fractions was detected with anti-myc antibody. The M_r ~88 000 kDa band is not present in lysate without plasmid (NT). Myc-Eps1 remains associated with membranes after extraction with high salt or high pH buffer. (**B**) Localization of Eps1 by indirect immunofluorescence. Upper panels: *eps1*Δ cells bearing *myc-EPS1* (pWQ29) were fixed for double staining with anti-myc and anti-Kar2, followed by Cy3- and Cy2-conjugated secondary antibodies. Arrows indicate co-localization. Lower panels: double staining of myc-Eps1 with HA-Pma1-D378N. Cells (WQY1) bearing *pMET-HA-pma1* (pWQ12) and *myc-EPS1* (pWQ29) growing exponentially in minimal medium containing 600 μM methionine were harvested, washed and resuspended in methionine-free medium to induce synthesis of mutant Pma1 (see Materials and methods). After 3 h, cells were prepared for staining with polyclonal anti-HA and monoclonal anti-myc antibodies.

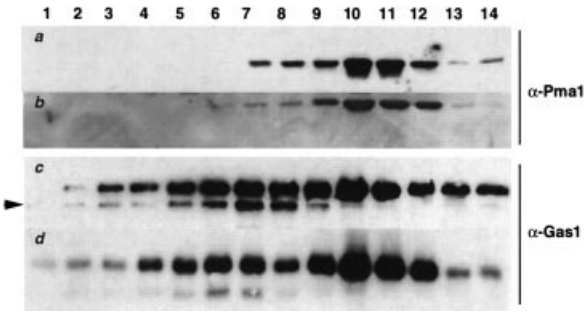

Fig. 10. Effect of *eps1* on protein export from the ER. Localization of Pma1 and Gas1 in wild-type (F1105) and *eps1* (WQY1) cells. Cell lysate was fractionated on a Renografin density gradient. Fractionation was analyzed by Western blotting with polyclonal anti-Pma1 and anti-Gas1 antibodies. In panels a and b, Pma1 is found predominantly in fraction 10 in *eps1* and wild-type cells, respectively. In panel c, in *eps1* cells, there is accumulation of the 105 kDa ER (arrowhead) form of Gas1 in fractions 7 and 8; in addition, the 125 kDa mature form is found in a peak in fraction 10. In panel d, the majority of Gas1 in wild-type cells is in fraction 10.

machinery (Hampton *et al*., 1996; Knop *et al*., 1996; McCracken *et al*., 1996; Loayza *et al*., 1998). Because the selection method for suppressors of *pma1-D378N* was based on the ability of the cells to grow (by delivering Pma1 to the cell surface), it was unlikely to yield mutants defective in degradation *per se*. Indeed, *eps1* cells stabilize Pma1-D378N by abolishing ER retention and allowing export of mutant and wild-type Pma1 to the cell surface (Figures 4 and 5).

We find that Eps1 is required for ER retention of Pma1-D378N but does not play an important role in normal retention of resident ER proteins (Figure 6). Moreover, Eps1 does not appear to play a role in the intracellular transport of wild-type Pma1 in the absence of Pma1-D378N (Figure 10). Therefore, *eps1*Δ does not appear to cause a general perturbation of protein trafficking.

Eps1 is a novel ER membrane protein containing a CXXC domain conserved in PDI family members (Figures 7and 9). Unlike *PDI1*, *EPS1* is not essential for cell viability. While the essential function of PDI to reshuffle non-native disulfide bonds is mediated by its thioredoxin domains (Luz and Lennarz, 1996; Wang and Tsou, 1998; Ferrari and Soling, 1999), it is not known how or whether the thioredoxin-like domain of Eps1 plays a role in ER quality control. If Eps1 interacts directly with Pma1-D378N, it is probably mediated by a domain other than the lumenal thioredoxin domain because topological predictions place only ~4% of Pma1 in the lumen (Serrano, 1989; Auer *et al*., 1998), and disulfide bonding does not appear to play any role in Pma1 structure or function (Petrov and Slayman, 1995). At present, we cannot rule out the possibility that ER export of Pma1-D378N is due to an indirect effect of *eps1*Δ, for instance, on the redox potential of the ER. Notably, however, folding and export of the redox-sensitive protein, CPY, is not perturbed detectably in *eps1* cells (Figure 8).

Although the means by which proteins are selected for ER-associated degradation is not known, it has been suggested that molecular chaperones might participate in identifying and delivering substrates to the degradation machinery (Hammond and Helenius, 1995; Brodsky and McCracken, 1997; Kopito, 1997; Sommer and Wolf,

1997). The observation that Eps1 is a member of the PDI family suggests a model in which Eps1 may have a chaperone-like function in recognition and retention of substrates for ER quality control. Indeed, it is becoming increasingly clear that members of the PDI family have chaperone functions in addition to their enzymatic activities (Luz and Lennarz, 1996; Wang and Tsou, 1998; Ferrari and Soling, 1999). Our hypothesis is consistent with the observation that ER-associated degradation of some substrates is inhibited in calnexin and BiP mutants (Plemper *et al*., 1997; Brodsky *et al*., 1999). Moreover, in this regard, it is of interest that in *eps1* cells there is a delay in export of newly synthesized Gas1, resulting in ER accumulation (Figure 10). This observation is consistent with a role for Eps1 in facilitating ER export of Gas1, although we cannot exclude the possibility that impairment of Gas1 export in *eps1* cells is indirect (Horvath *et al*., 1994).

While the molecular mechanism of Eps1 action awaits further work, its absolute requirement in retention and degradation of Pma1-D378N points to an important function in ER quality control.

Materials and methods

Media and strains

Unless specified, experiments were performed using strains isogenic with W303 (*MAT*α *ura3-1 leu2-3,112 his3-11,15 trp1-1 ade2-1 can1-100;* F1105, Fink laboratory collection, Whitehead Institute, Cambridge, MA). WQY1 (*MAT*α *ura3-1 leu2-3,112 his3-11,15 trp1-1 ade2-1 can1-100 eps1::HIS3*) was generated by transforming F1105 with pWQ10. MY3331 (*MAT*α *suc2 ura3-52 leu2-3, 112 his4-519 erd2-B25*) comes from M.Rose (Princeton University, NJ). MHY552 (*MAT*α *his3*Δ*200 leu2-3,112 ura3-52 lys2-801 trp1-1 ubc6*Δ*1::HIS3 ubc7::LEU2*) and sub62 (*MATa his3*Δ*200 leu2-3, 112 ura3-52 lys2-801 trp1-1*) were from M.Hochstrasser via D.Kornitzer (Technion, Haifa, Israel).

Standard yeast media and genetic manipulations were as described (Sherman *et al*., 1986). To study proteins under the control of a galactose-dependent promoter, cells were grown in synthetic complete medium containing 2% raffinose (in which there is neither induction nor inhibition of *GAL1*). Exponentially growing cells were then transferred to synthetic complete medium containing 2% galactose. After induction, synthesis was terminated by addition of glucose to 3%. Pma1-D378N under the control of the *MET25* promoter (Mumberg *et al*., 1994) behaves like that under *GAL1* control. To study these cells under repressing conditions, cells were grown in minimal medium containing 600 μM methionine. To induce synthesis of mutant Pma1, cells were harvested, washed once with water, and placed in minimal medium without methionine; to shut off synthesis, 2 mM methionine was added.

Plasmids and molecular biology

B2513 is a *URA3*-marked centromeric plasmid containing HA-tagged *SHR3* (Ljungdahl *et al*., 1992; Fink laboratory collection). The plasmid pXZ28, obtained from J.Haber (Brandeis University, Waltham, MA), contains a *URA3* marker and *PMA1* under the control of a galactose-inducible promoter; *PMA1* is tagged with an HA epitope introduced after the second amino acid (Harris *et al*., 1994). pRN409L and pRN409U are *LEU2*- and *URA3*-marked plasmids, respectively, containing the *pma1-D378N* mutation within a 3.8 kb *Hin*dIII–*Sac*I fragment from p*PMA1*.2 (Nakamoto *et al*., 1998); *pma1* is under the control of the *GAL1* promoter. pFT4 carries *PMA1* with a c-myc epitope introduced after the second amino acid. pRN409 and pFT4 were provided by C.Slayman (Yale University, New Haven, CT). pWQ2 bearing *myc-pma1-D378N* was constructed by replacing the 750 bp *Hin*dIII–*Bst*EII fragment of pRN409L with that of pFT4; the *Hin*dIII site in both plasmids was introduced at –27 from the start codon of *PMA1* (Nakamoto *et al*., 1991). pWQ12 contains *HA-pma1-D378N* cloned after the *MET25* promoter. pWQ12 was constructed by first cloning a 3.7 kb *Hin*dIII–*Sma*I fragment bearing *myc-pma1-D378N* from pWQ2 into pBSII (KS^+) (Stratagene, La Jolla, CA), followed by excision of the fragment using *Hin*dIII and *Xho*I sites for cloning into FB1521, a *URA3*-marked centromeric plasmid bearing the *MET25* promoter (Mumberg *et al*., 1994), generating pWQ5. To replace the myc tag with an HA tag, the plasmid pND542 (derived from pXZ28, provided by N.Davis, Wayne State University, MI) was used as a template for PCR. A fragment of 0.8 kb was amplified using the oligonucleotide TCCCCCGGGAGCTAGTTAAAGAAAATC to introduce a *Sma*I site at –67 bp from the start codon and the oligonucleotide CCTTCACCTCTCTTAACA. After cutting with *Sma*I and *Bst*EII, the PCR fragment was used to replace the corresponding fragment in pWQ5.

The plasmid pWQ10 to disrupt *EPS1* was constructed by using PCR to amplify genomic DNA; a 1.5 kb PCR product with introduced *Eco*RI and *Sma*I restriction sites upstream of the *EPS1* start codon and a 1.5 kb product with introduced *Sma*I–*Xba*I sites downstream of the stop codon were cloned in pBSII; to mark the disruption, a 3.1 kb fragment containing *HIS3* and kan^r (from B2179, Fink laboratory collection) was inserted at *Sma*I.

For the plasmid shuffle experiment, pWQ19 was constructed by amplifying genomic DNA by PCR using an oligonucleotide to introduce a *Sal*I site ~1 kb upstream of the *EPS1* start codon (AAGTCGACCCTCGGTGAGCACCCCAC) and another oligo at the stop codon. The product was subcloned into a *LEU2*-marked 2μ vector (B2201; Fink laboratory collection) via pGEM-T Easy (Promega, Madison, WI) at *Sal*I–*Not*I. The multicopy *EUG1* plasmid, pCT44, also used for plasmid shuffle, was from Tom Stevens' laboratory (Tachibana and Stevens, 1992). To place an epitope tag at the C-terminus of Eps1 prior to the putative KKKNQD retrieval signal, pWQ26 was constructed by amplifying genomic DNA by PCR using the oligonucleotide annealing ~1 kb upstream of the start codon and the oligonucleotide GCCAGAAGATCTGGGATC; the 3.3 kb product was then cut with *Sal*I and *Bgl*II and ligated to the *Sal*I–*Bam*HI sites of pRS316 (Sikorski and Hieter, 1989). pWQ26 was used as a template for oligonucleotide-directed mutagenesis (Kunkel *et al*., 1987) using TTGATTTTTTTTTTGGATCCCTCCATATTTCC to introduce a *Bam*HI site into which three tandem copies of a myc epitope was cloned to generate pWQ28. pWQ29 and pWQ30 are 2μ vectors marked with *LEU2* (B2201) and *URA3* (pRS202), respectively, bearing *EPS1-myc*.

Genetic selection

F1105 cells bearing *pGAL-pma1-D378N* (pRN409U) were transformed with each of 14 independent pools of a mutagenized genomic library containing random *lacZ* and *LEU2* insertions (Burns *et al*., 1994). Leu^+ Ura^+ transformants (~88 000) were plated on synthetic complete media without leucine and uracil, containing 2% galactose. Ninety six colonies that grew on galactose medium were crossed to 10556-20A (*MATa, ura3-1, leu2-3,112, his3-11,15, trp1-1, can1-100*; Fink laboratory collection), and the diploid was subjected to tetrad analysis to determine whether the ability to grow in the presence of *pGAL-pma1-D378N* was linked to a single *LEU2* insertion. Seventeen of the Leu^+ Ura^+ transformants fulfilled these criteria, and sequence analysis of genomic DNA adjacent to the insertion in these strains was undertaken as described (Burns *et al*., 1994). DNA sequencing was performed by the AECOM DNA sequencing facility. Sequences were analyzed using BLAST (Altschul *et al*., 1990). Insertion of *lacZ* in the *eps1*::*LEU2* mutant is at codon 1810 out of a total of 2106 codons.

Indirect immunofluorescence

Indirect immunofluorescence staining was performed essentially as described (Rose *et al*., 1990). Briefly, cultures growing exponentially in medium containing 2% galactose were harvested and fixed in 4.4% formaldehyde, 0.1 M K phosphate, pH 6.5 for 2 h at room temperature. Cells were spheroplasted with oxalyticase (Enzogenetics, Corvallis, OR), and permeabilized with methanol and acetone. Cells were then incubated overnight with monoclonal or polyclonal anti-HA (BAbCo, Berkeley, CA), monoclonal anti-myc (Santa Cruz Biotechnology Inc.) and/or anti-Kar2 antibody (provided by Mark Rose, Princeton, NJ). Primary antibody staining was visualized with Cy2- and/or Cy3-conjugated secondary antibodies (Amersham, Arlington Heights, IL, and Jackson Immuno-Research, West Grove, PA). Experiments for Figure 4 were photographed using a Zeiss Axiophot microscope. All other experiments were visualized using an Olympus IX70 microscope, images were collected digitally, and adjusted with Adobe Photoshop.

Cell fractionation, Western blot and metabolic labeling

Cell fractionation on Renografin density gradients was performed essentially as described (Schandel and Jenness, 1994; Jenness *et al*., 1997). Briefly, cell lysates were prepared by suspending cells in buffer (50 mM

Tris, pH 7.5, 1 mM EDTA) in the presence of a protease inhibitor cocktail including 1 mM phenylmethylsulfonyl fluoride (PMSF) (Chang and Slayman, 1991) and vortexing with glass beads. Unbroken cells were removed by centrifugation at 400 *g* for 5 min. Lysate (0.5 ml) was mixed with 0.5 ml Renografin-76 (a gift from L.Marsh, Albert Einstein College of Medicine), placed at the bottom of a centrifuge tube and overlaid with 1 ml of 34, 30, 26 and 22% Renografin solutions (prepared by diluting Renografin-76 with Tris-EDTA buffer). Gradients were centrifuged in an SW50.1 rotor overnight at 150 000 *g* at 4°C. Fractions (350 µl) were collected from the top of each gradient. To prevent Renografin from interfering with subsequent Western blots, aliquots of each fraction (150 µl) were diluted with Tris-EDTA buffer containing protease inhibitors (1.5 ml), and membranes were pelleted by centrifugation at 100 000 *g* for 1 h. For Western blot of cell lysate, cells were broken by vortexing with glass beads as described (Chang and Slayman, 1991), and samples were normalized to protein using the Bradford assay (Bio-Rad Laboratories, Hercules, CA). After separation by SDS–PAGE and electrophoretic transfer to nitrocellulose, Western blots were performed using anti-HA, anti-myc, anti-Sec61 (provided by R.Schekman, University of California, Berkeley, CA) and anti-Gas1 (provided by T.Doering, Cornell University School of Medicine, NY).

For metabolic labeling experiments involving *pGAL-pma1-D378N*, cells were grown to mid-log in synthetic complete medium without methionine and cysteine and containing 2% raffinose, and then resuspended in fresh medium containing 2% galactose. For experiments with *pMET-pma1-D378N*, cells were grown to mid-log in minimal medium containing 600 µM methionine, harvested, washed and resuspended in methionine-free medium for 2 h. Cells were labeled with Expre^{35}S^{35}S (2 mCi/25 OD_{600} cells) and chased in the presence of 10 mM methionine and cysteine. At various times of chase, aliquots were placed on ice in the presence of 10 mM Na azide. Cell lysate was prepared by vortexing with glass beads. For immunoprecipitation, lysate samples were normalized to acid-precipitable c.p.m. Immunoprecipitations were performed in RIPA buffer, and analyzed by SDS–PAGE and fluorography. Polyclonal anti-CPY was provided by T.Stevens (University of Oregon, Eugene, OR).

Acknowledgements

We thank Carolyn Slayman, James Haber, Mark Rose, Randy Schekman, Daniel Kornitzer, Tamara Doering, William Lennarz and Tom Stevens for plasmids, antibodies and strains. We thank Peter Arvan for helpful discussion and comments on the manuscript. This work was supported by a grant from the NIH (GM 58212).

References

Altschul,S.F., Gish,W., Miller,W., Myers,E.W. and Lipman D.J. (1990) Basic local alignment tool. *J. Mol. Biol.*, **215**, 403–410.

Auer,M., Scarborough,G.A. and Kuhlbrandt,W. (1998) Three-dimensional map of the plasma membrane H^+-ATPase in the open conformation. *Nature*, **392**, 840–843.

Benito,B., Moreno,E. and Losario,R. (1991) Half-life of plasma membrane ATPase and its activating system in resting yeast cells. *Biochim. Biophys. Acta*, **1063**, 265–268.

Boeke,J.D., Trueheart,J., Natsoulis,G. and Fink,G.R. (1987) 5-Fluoroorotic acid as a selective agent in yeast molecular genetics. *Methods Enzymol.*, **154**, 164–175.

Brodsky,J.L. and McCracken,A.A. (1997) ER-associated and proteasome-mediated protein degradation: how two topologically restricted events came together. *Trends Cell Biol.*, **7**, 151–156.

Brodsky,J.L., Werner,E.D., Dubas,M.E., Goeckeler,J.L., Kruse,K.B. and McCracken,A.A. (1999) The requirement for molecular chaperones during endoplasmic reticulum-associated protein degradation demonstrates that protein export and import are mechanistically distinct. *J. Biol. Chem.*, **274**, 3453–3460.

Burns,N., Grimwade,B., Ross-Macdonald,P.B., Choi,E.-Y., Finberg,K., Roeder,G.S. and Snyder,M. (1994) Large-scale analysis of gene expression, protein localization and gene disruption in *Saccharomyces cerevisiae. Genes Dev.*, **8**, 1087–1105.

Chang,A. and Fink,G.R. (1995) Targeting of the yeast plasma membrane [H^+]ATPase: a novel gene *AST1* prevents mislocalization of mutant ATPase to the vacuole. *J. Cell Biol.*, **128**, 39–49.

Chang,A. and Slayman,C.W. (1991) Maturation of the yeast plasma membrane [H^+]ATPase involves phosphorylation during intracellular transport. *J. Cell Biol.*, **115**, 289–295.

Cherry,J.M., Adler,C., Ball,C., Dwight,S., Chervitz,S., Juvik,G., Weng,S. and Botstein,D. (1997) *Saccharomyces* Genome Database (http://genome-www.stanford.edu/Saccharomyces).

de-Kerchove d'Exaerde,A., Supply,P. and Goffeau,A. (1996) Subcellular traffic of the plasma membrane H^+-ATPase in *Saccharomyces cerevisiae*. *Yeast*, **12**, 907–916.

DeWitt,N.D., Tourinho dos Santos,C.F., Allen,K.E. and Slayman,C.W. (1998) Phosphorylation region of the yeast plasma-membrane H^+-ATPase. Role in protein folding and biogenesis. *J. Biol. Chem.*, **273**, 21744–21751.

Doering,T.L. and Schekman,R. (1996) GPI anchor attachment is required for Gas1p transport from the endoplasmic reticulum in COPII vesicles. *EMBO J.*, **15**, 182–191.

Ferrari,D.M. and Soling,H.-D. (1999) The protein disulphide-isomerase family: unraveling a string of folds. *Biochem. J.*, **339**, 1–10.

Gething,M.-J. and Sambrook,J. (1992) Protein folding in the cell. *Nature*, **355**, 33–45.

Gunther,R., Brauer,C., Janetzky,J., Forster,H.-H., Ehbrecht,E.-M., Lehle,L. and Kuntzel,H. (1991) The *Saccharomyces cerevisiae TRG1* gene is essential for growth and encodes a lumenal endoplasmic reticulum glycoprotein involved in the maturation of vacuolar carboxypeptidase. *J. Biol. Chem.*, **266**, 24557–24563.

Hammond,C. and Helenius,A. (1995) Quality control in the secretory pathway. *Curr. Opin. Cell Biol.*, **7**, 523–529.

Hampton,R.Y., Gardner,R.G. and Rine,J. (1996) Role of 26S proteasome and *HRD* genes in the degradation of 3-hydroxy-3-methylglutaryl-CoA reductase, an integral endoplasmic reticulum membrane protein. *Mol. Biol. Cell*, **7**, 2029–2044.

Harris,S.L., Na,S., Zhu,X., Seto-Young,D., Perlin,D., Teem,J.H. and Haber,J.E. (1994) Dominant lethal mutations in the plasma membrane H^+-ATPase gene of *Saccharomyces cerevisiae. Proc. Natl Acad. Sci. USA*, **91**, 10531–10535.

Higgins,D.G., Bleasby,A.J. and Fuchs,R. (1992) CLUSTAL V: improved software for multiple sequence alignment. *Comp. Appl. Biosci.*, **8**, 189–191.

Horvath,A., Sutterlin,C., Manning-Krieg,U., Movva,N.R. and Riezman,H. (1994) Ceramide synthesis enhances transport of GPI-anchored proteins to the Golgi apparatus in yeast. *EMBO J.*, **13**, 3687–3695.

Jackson,M.R., Nilsson,T. and Peterson,P.A. (1990) Identification of a consensus motif for retention of transmembrane proteins in the endoplasmic reticulum. *EMBO J.*, **9**, 3153–3162.

Jenness,D.D., Li,Y., Tipper,C. and Spatrick,P. (1997) Elimination of defective α-factor pheromone receptors. *Mol. Cell. Biol.*, **17**, 6236–6245.

Knop,M., Finger,A., Braun,T., Hellmuth,K. and Wolf,D.H. (1996) Der1, a novel protein specifically required for endoplasmic reticulum degradation in yeast. *EMBO J.*, **15**, 753–763.

Kopito,R. (1997) ER quality control: the cytoplasmic connection. *Cell*, **88**, 427–430.

Kunkel,T.A., Roberts,J.D. and Zakour,R.A. (1987) Rapid and efficient site-specific mutagenesis without phenotypic selection. *Methods Enzymol.*, **154**, 508–519.

LaMantia,M., Miura,H., Tachikawa,H., Kaplan,A., Lennarz,W.J. and Mizunaga,T. (1991) Glycosylation site binding protein and protein disulfide isomerase are identical and essential for cell viability in yeast. *Proc. Natl Acad. Sci. USA*, **88**, 4453–4457.

Ljungdahl,P.O., Gimeno,C.J., Styles,C.A. and Fink,G.R. (1992) *SHR3*: a novel component of the secretory pathway specifically required for localization of amino acid permeases. *Cell*, **71**, 463–478.

Loayza,D., Tam,A., Schmidt,W.K. and Michaelis,S. (1998) Ste6p mutants defective in exit from the endoplasmic reticulum (ER) reveal aspects of an ER quality control pathway in *Saccharomyces cerevisiae. Mol. Biol. Cell*, **9**, 2767–2784.

Luz,J.M. and Lennarz,W.J. (1996) Protein disulfide isomerase: a multifunctional protein of the endoplasmic reticulum. *EXS*, **77**, 97–117.

Maldonado,A.M., de la Fuente,N. and Portillo,F. (1998) Characterization of an allele-nonspecific intragenic suppressor in the yeast plasma membrane H^+-ATPase gene (*PMA1*). *Genetics*, **150**, 11–19.

McCracken,A.A., Karpichev,I.V., Ernaga,J.E., Werner,E.D., Dillin,A.G. and Courchesne,W.E. (1996) Yeast mutants deficient in ER-associated degradation of the Z variant of α-1-protease inhibitor. *Genetics*, **144**, 1355–1362.

Mumberg,D., Muller,R. and Funk,M. (1994) Regulatable promoters of *Saccharomyces cerevisiae*: comparison of transcriptional activity and their use for heterologous expression. *Nucleic Acids Res.*, **22**, 5767–5768.

Nakamoto,R.K., Rao,R. and Slayman,C.W. (1991) Expression of the yeast plasma membrane [H^+]ATPase in secretory vesicles: a new strategy for directed mutagenesis. *J. Biol. Chem.*, **266**, 7940–7949.

Nakamoto,R.K., Verjovski-Almeida,S., Allen,K.E., Ambesi,A., Rao,R and Slayman,C.W. (1998) Substitutions of aspartate 378 in the phosphorylation domain of the yeast *PMA1* H^+-ATPase disrupt protein folding and biogenesis. *J. Biol. Chem.*, **273**, 7338–7344.

Petrov,V.V. and Slayman,C.W. (1995) Site-directed mutagenesis of the yeast *PMA1* H^+-ATPase; structural and functional role of cysteine residues. *J. Biol. Chem.*, **270**, 28535–28540.

Plemper,R.K., Bohmler,S., Bordallo,J., Sommer,T. and Wolf,D. (1997) Mutant analysis links the translocon and BiP to retrograde protein transport for ER degradation. *Nature*, **388**, 891–895.

Roberg,K. Crotwell,J.M., Espenshade,P., Gimeno,R. and Kaiser,C.A. (1999) *LST1* is a *SEC24* homologue used for selective export of the plasma membrane ATPase from the endoplasmic reticulum. *J. Cell Biol.*, **145**, 659–672.

Rose,M.D., Misra,L.M. and Vogel,J.P. (1989) *KAR2*, a karyogamy gene, is the yeast homolog of the mammalian BiP/GRP78 gene. *Cell*, **57**, 1211–1221.

Rose,M.D., Winston,F. and Hieter,P. (1990) *Methods in Yeast Genetics*. Cold Spring Harbor Laboratory Press, Cold Spring Harbor, NY, pp. 198.

Schandel,K.A. and Jenness,D.D. (1994) Direct evidence for ligand-induced internalization of the yeast α-factor pheromone receptor. *Mol. Cell. Biol.*, **14**, 7245–7255.

Semenza,J.C., Hardwick,K.G., Dean,N. and Pelham,H.R. (1990) *ERD2*, a yeast gene required for the receptor-mediated retrieval of lumenal ER proteins from the secretory pathway. *Cell*, **61**, 1349–1357.

Serrano,R. (1989) Structure and function of plasma membrane ATPase. *Annu. Rev. Plant Physiol.*, **40**, 61–94.

Sherman,F.,. Hicks,J.B. and Fink,G.R. (1986) *Methods in Yeast Genetics: A Laboratory Manual*. Cold Spring Harbor Laboratory Press, Cold Spring Harbor, NY, pp. 523–585.

Sikorski,R.S. and Hieter,P. (1989) A system of shuttle vectors and yeast host strains designed for efficient manipulation of DNA in *Saccharomyces cerevisiae. Genetics*, **122**, 19–27.

Sommer,T. and Wolf,D.H. (1997) Endoplasmic reticulum degradation: reverse protein flow of no return. *FASEB J.*, **11**, 1227–1233.

Steck,T.L. and Yu,J. (1973) Selective solubilization of proteins from red blood cell membranes by protein perturbants. *J. Supramol. Struct.*, **1**, 220–232.

Stevens,T., Esmon,B. and Schekman,R. (1982) Early stages in the yeast secretory pathway are required for transport of carboxypeptidase Y to the vacuole. *Cell*, **30**, 439–448.

Sutterlin,C., Doering,T.L., Schimmoller,F., Schroder,S. and Riezman,H. (1997) Specific requirements for the ER to Golgi transport of GPI-anchored proteins in yeast. *J. Cell Sci.*, **110**, 2703–2714.

Tachibana,C. and Stevens,T.H. (1992) The yeast *EUG1* gene encodes an endoplasmic reticulum protein that is functionally related to protein disulfide isomerase. *Mol. Cell. Biol.*, **12**, 4601–4611.

Tachikawa,H., Funahashi,W., Takeuchi,Y., Nakanishi,H., Nishihara,R., Katoh,S., Gao,X., Mizunaga,T. and Fujimoto,D. (1997) Overproduction of Mpd2p suppresses the lethality of protein disulfide isomerase depletion in a CXXC sequence dependent manner. *Biochem. Biophys. Res. Commun.*, **239**, 710–714.

Tachikawa,H., Takeuchi,Y., Funahashi,W., Miura,T., Gao,X., Fujimoto,D., Mizunaga,T. and Onodera,K. (1995) Isolation and characterization of a yeast gene, *MPD1*, the overexpression of which suppresses inviability caused by protein disulfide isomerase depletion. *FEBS Lett.*, **369**, 212–216.

Wang,C.-C. and Tsou,C.-L. (1998) Enzymes as chaperones and chaperones as enzymes. *FEBS Lett.*, **425**, 382–384.

Received April 26, 1999; revised September 7, 1999; accepted September 8, 1999